

Cellular uptake and imaging studies of glycosylated silica nanoprobe (GSN) in human colon adenocarcinoma (HT 29 cell line)

Bitā Mehravi¹

Mohsen Ahmadi¹

Massoud Amanlou²

Ahmad Mostaar¹

Mehdi Shafiee Ardestani³

Negar Ghalandarlaki⁴

¹Biomedical Engineering and Medical Physics Department, Faculty of Medicine, Shahid Beheshti University of Medical Sciences, Tehran, Iran;

²Department of Medicinal Chemistry, Faculty of Pharmacy and Drug Design and Development Research Center, Tehran University of Medical Sciences, Tehran, Iran; ³Department of Radiopharmacy, Faculty of Pharmacy, Tehran University of Medical Sciences, Tehran, Iran; ⁴Department of Biological Science, School of Science, Science and Research branch, Islamic Azad University, Tehran, Iran

Correspondence: Mohsen Ahmadi
Biomedical Engineering and Medical Physics Department,
Faculty of Medicine, Shahid Beheshti University of Medical Sciences, Velenjak Street, Shahid Chamran Highway, Tehran, Iran
Tel +98 212 243 9941
Fax +98 212 243 9941
Email dr.mohsen.ahmadi@gmail.com

Massoud Amanlou
The Department of Medicinal Chemistry, Faculty of Pharmacy and Drug Design and Development Research Center,
PO Box 14155-6451,
Tehran University of Medical Sciences, Tehran, Iran
Tel +98 216 695 9067
Fax +98 216 412 1111
Email amanlou@tums.ac.ir

Purpose: In recent years, molecular imaging by magnetic resonance imaging (MRI) has gained prominence in the detection of tumor cells. The scope of this study is on molecular imaging and on the cellular uptake study of a glycosylated silica nanoprobe (GSN).

Methods: In this study, intracellular uptake (HT 29 cell line) of GSN was analyzed quantitatively and qualitatively with inductively coupled plasma atomic emission spectroscopy, flow cytometry, and fluorescent microscopy. In vitro and in vivo relaxometry of this nanoparticle was determined using a 3 Tesla MRI; biodistribution of GSN and Magnevist® were measured in different tissues.

Results: Results suggest that the cellular uptake of GSN was about 70%. The r_1 relaxivity of this nanoparticle in the cells was measured to be $12.9 \pm 1.6 \text{ mM}^{-1} \text{ s}^{-1}$ and on a per lanthanide gadolinium (Gd^{3+}) basis. Results also indicate an average cellular uptake of $0.7 \pm 0.009 \text{ pg Gd}^{3+}$ per cell. It should be noted that 3-(4,5-Dimethylthiazol-2-yl)-2,5-diphenyltetrazolium bromide (MTT) assay demonstrated that the cells were effectively labeled without cytotoxicity, and that using MRI for quantitative estimation of delivery and uptake of targeted contrast agents and early detection of human colon cancer cells using targeted contrast agents, is feasible.

Conclusion: These results showed that GSN provided a critical guideline in selecting these nanoparticles as an appropriate contrast agent for nanomedicine applications.

Keywords: cellular uptake, contrast agent, glucosamine, mesoporous silica nanospheres, molecular imaging, MRI

Introduction

Colon cancer is the second leading cause of death from cancer in the United States.¹ The American Cancer Society estimates that in 2012, 103,170 men and women (49,920 men and 53,250 women) will be diagnosed with colon cancer and that 51,960 men and women (26,470 men and 25,220 women) will die of colon cancer.¹

Efficient treatment of colon cancer cells depends on the early diagnosis of the disease. Magnetic resonance imaging (MRI) is a powerful tool for imaging cancer tissues.² Contrast agents are used to enhance soft tissues. The major barriers to the development of MRI contrast agents are low specificity to the desired tissues and potential toxicity, so designing an MRI contrast agent with unique physiochemical properties that can be up taken selectively by cancer cells and be detected at the single-cell level is essential.³

Mesoporous silica nanospheres (MSN) have several attractive properties such as large surface areas and porous interiors that can be used to store various molecules.⁴ In addition, their pore size and their size and shape can be easily modified, making

them a suitable choice as intracellular contrast agents or drug carriers.⁵ MSNs have an internal surface and an external surface; these characteristics make MSN easily multifunctional, which is the reason why these materials are used for targeting specific cells and organs in the body.⁴ Grafting of targeting groups on the surface of MSN can be used to increase the specific accumulation of these mesoporous materials in cancer tissue.^{5–7} Several research groups have developed different strategies to prepare nanoparticles functionalized to intervene in biological processes;^{8–10} glucose is one of these groups for targeting cancer cells.^{10–13} Cancer cells have an increased demand for glucose compared to normal cells.⁸ This demand is met through enhanced cellular uptake of glucose through the upregulation of specific transporters.^{5,8} The transport of glucose into cancer cells is mediated by specific membrane proteins called transporters. The upregulation of these transporters correlates with the higher transport of glucose to cancer cells.⁸ The increased glucose uptake by the tumor is often exploited for tumor detection. The 2-fluoro-2-deoxy-D-glucose molecule (¹⁸FDG) is a glucose analog that is most commonly used in positron emission tomography imaging.¹⁴

In this study, a novel nanoprobe was designed and synthesized that can be monitored inside colon cancer cells by both MRI and fluorescence imaging methods. The targeting ligand modification increased the uptake of this glyconanoprobe by colon cancer cells when compared to noncancer cells. This glyconanoprobe's potential to be used in the imaging of the targeted cell of a tissue is beneficial for both imaging purposes and for the treatment of cancer in its early stages.

Material and methods

Materials

The tetraethylorthosilicate (98%), $\text{GdCl}_3 \cdot 6\text{H}_2\text{O}$ (99%), anhydrous ethanol (99.5%), methanol sodium hydroxide (NaOH), bromoacetic acid, cetyltrimethylammonium bromide (CTAB, 98%), 3-aminopropyl triethoxysilane (APTES, 99%), and 3-(trimethoxysilylpropyl) diethylenetriamine, anhydrous N,N-dimethylformamide (DMF, 99.8%), toluene (99.8%), [4-(2-hydroxyethyl)-1-piperazineethanesulfonic acid] (HEPES), Tween[®] 20, phosphate buffered saline (PBS), and rhodamine B isothiocyanate were purchased from Sigma-Aldrich (St Louis, MO, USA), and used without further purification. In addition, 3-(trimethoxysilylpropyl) diethylenetriamine was obtained from Gelest, Inc. (Morrisville, PA, USA). N-5-azido-2-nitrobenzoyloxysuccinimide (ANB-NOS) was purchased from Pierce (Thermo Fisher Scientific, Waltham, MA, USA). A dialysis bag

with a 500–1000 D cut-off was obtained from Spectrum[®] Laboratories, Inc. (Rancho Dominguez, CA, USA). Other materials were purchased from Merck (Merck KGaA, Darmstadt, Germany). Fetal bovine serum (Invitrogen, Beijing, People's Republic of China) and penicillin–streptomycin were also purchased from Sigma-Aldrich.

The human colon adenocarcinoma cell line (HT 29) was purchased from the National Cell Bank of Pasteur Institute, Iran. The BALB/c mice were purchased from the Laboratory Animal Center Institute of Cancer Research, Tehran University of Medical Sciences, Iran.

Instrumentation

The lanthanide gadolinium (Gd^{3+}) ions were quantified using an inductively coupled plasma atomic emission spectrometer (ICP-AES) (Optima 2300; PerkinElmer, Waltham, MA, USA). The zeta-potential of the MSN- Gd^{3+} -DG dispersed in an aqueous solution (pH = 7–8) was measured using a Zetasizer analyzer (Malvern Instruments, Malvern, UK). MR images were acquired on a Siemens (Erlangen, Germany) and 3 Tesla MRI.

Flow cytometry analyses were performed with an Epics Altra HyPerSort flow cytometer (Beckman Coulter, Brea, CA, USA) with an air-cooled argon ion laser (488 nm, 15 mW). This standard instrument is equipped with two light scatter detectors that measure forward scatter (FSC) and side scatter. The data were analyzed using Coulter software. The absorbance was measured at 450 nm with BioTek absorbance microplate readers (ELX800; BioTek Instruments, Inc, Winooski, VT, USA).

GSN synthesis

The glycosylated silica nanoprobe (GSN) was synthesized according to our previous report.¹⁵ Briefly, MSN (1.0 g) were synthesized using a surfactant template, base-catalyzed condensation, according to the Stöber method. Amino-functionalized silica nanospheres (MSN- NH_2) (2.0 g) were prepared by silanization with APTES (2.0 g) in 200 mL water for 6 hours.¹⁵ The MSN (1.5 g) were refluxed in a 162 mL methanol solution of hydrochloric acid (1.57 M) for 12 hours to remove the CTAB surfactant. The Gd^{3+} -Si-diethylenetriamine tetraacetic acid (DTTA) complex (0.5 mL, 0.1 M) was loaded in surfactant-extracted MSN (200.0 g) via siloxane linkage by refluxing in toluene. ANB-NOS were dissolved in DMF. MSN- NH_2 (500.0 mg) and ANB-NOS (50.0 mg) were reacted in 20 mM of HEPES at a pH of 8 for 2 hours at room temperature, in darkness. The MSN-ANB-NOS (100.0 mg) was saturated by incubation at 37°C for 30 minutes, with an excess amount of glucosamine. The glucosamine was attached to the MSN surfaces by exposing

them to 302 nm of light for 5 minutes at room temperature. Unbound glucosamine molecules were removed by washing them three times with a phosphate buffer (pH = 7.5) containing 0.05% Tween® 20; this was dialyzed against PBS to ensure the removal of any free glucosamine (500–1000 D cutoff).

Preparation of fluorescent-doped glycosylated silica nanosphere (GSNF)

Rhodamine B isothiocyanate (7.0 mg) was dissolved in absolute ethanol (5.0 mL), and APTES (4.0 μ L) was added to the solution. The reaction mixture was stirred at room temperature, in darkness, and under N₂, for 24 hours.¹⁶ Silica mesoporous nanospheres –NH₂ (50 mg) were suspended in dried toluene (5.0 mL). Then a solution of rhodamine-APS (100.0 μ L, 6 mM) was added. The mixture was refluxed overnight. NH₂-SN-FITC (Fluorescent -doped Amino Fractionalized Mesoporous Silica Nanospheres) was isolated by centrifuging, and it was washed with water and ethanol twice.

MSN-NH₂-FITC (500.0 mg) and ANB-NOS (50.0 mg) were reacted in 20 mM of HEPES at a pH of 8 for 2 hours at room temperature, in darkness. The MSN-FITC-ANB-NOS (100.0 mg) were saturated by incubation at 37°C for 30 minutes with an excess amount of glucosamine. The glucosamine was attached to the MSN-FITC surfaces by exposing them to 302 nm of light for 5 minutes at room temperature.

Cell culture and silica nanosphere labeling

The human colon adenocarcinoma cell line (HT 29) was purchased from the National Cell Bank of Pasteur Institute of Iran. The cells (2×10^6) were cultured at 37°C and at 5% CO₂ using standard cell culture media, containing Dulbecco's Modified Eagle's medium (DMEM). The cell culture medium was supplemented with 10% fetal bovine serum and 1% penicillin–streptomycin.

For GSN labeling, 2×10^6 cells per well were plated in six-well plates for 24 hours, and after incubation (1 hour) were plated with the GSN (75 μ g mL⁻¹) for 1 hour. Labeled cells were then washed twice with PBS to remove any excess caron nano tubes that might be adsorbed on the cell membrane. Then, the cellular uptake of Gd³⁺ ions was analyzed by ICP-AES (Optima 3100XL; PerkinElmer), quantitatively. The analyses were performed in triplicates and the means \pm standard deviations of the results were calculated.

For the GSN-labeling, the cells were subcultured every 72 hours, and they were harvested when they reached 70% of confluency using 0.05% trypsin–ethylenediaminetetraacetic acid. The cells were cultured at a density of 2×10^6 cells/well in 96-well plates for the following experiments.^{17,18}

MTT assay

It should be noted that a 3-(4,5-Dimethylthiazol-2-yl)-2,5-diphenyltetrazolium bromide (MTT)-based cell proliferation assay was used to determine the highest concentration of GSN solution suspension that could be used for cell labeling without significant cytotoxicity. To do so, HT 29 cells were incubated with various amounts of GSN (10 μ g mL⁻¹, 30 μ g mL⁻¹, 60 μ g mL⁻¹, and 90 μ g mL⁻¹) in a 96-well microplate for 24 hours, using unlabeled cells as control. Each concentration was tested in triplicate. The cells were washed with PBS before the addition of MTT to each well. After 4 hours, the absorbance of purple formazone was measured using BioTek's absorbance microplate reader at 450 nm.¹⁰

Flow cytometry

Flow cytometry was performed with a FAC Scan Cytometer equipped with Cell Quest Software (Becton Dickinson Immunocytometry System; BD Biosciences, San Jose, CA, USA), by counting 30,000 events, and data were analyzed using WinMDI software. The experiments were performed as follows: 5×10^5 cells were washed twice with 500 μ L buffer by centrifugation (2000 rpm for 10 minutes) and reconstituted in 100.0 μ L of buffer. Then, 100.0 μ L of GSN-FITC (fluorescent-doped glycosylated silica nanosphere) was added and incubated with cells for 1 hour. Cells were washed twice and reconstituted in 200.0 μ L of buffer. GSN-FITCs were directly detected by flow cytometry.¹⁹

Fluorescence staining and microscopy

Following this, 5×10^5 cells were seeded per well in 6-well plates, in 3 mL of culture medium to allow for attachment. After 24 hours, cells were incubated with GSNF for 1 hour. After that, the growth medium was removed, and the cells were then washed three times with PBS and fixed with PBS solution of 4% formaldehyde. Cellular uptake was observed using a fluorescence microscopy (Olympus IX51; Olympus Corporation, Tokyo, Japan).

In vitro MRI phantom preparation

HT 29 cells (1×10^5) were incubated with different doses of GSN for 1 hour. The labeled cells were washed with PBS and the cells were trypsinized and resuspended in an equal volume of DMEM culture media and 2% of agarose gel (Sigma-Aldrich) at 37°C. Cells were then transferred immediately to 1 mL syringes to prepare MRI phantom; the relaxation times were measured. The unlabeled cells were used as the control group. For quantitative data analysis, obtained MRI images were transferred by DICOM software

V 1.3.5 (Digital Imaging and Communications in Medicine, Rosslyn, VA, USA).¹⁸

In another experiment, four different concentrations of labeled cell phantoms (1×10^6 , 3×10^6 , 5×10^6 , and 7×10^6 cells) were labeled with the same GNS concentration ($75 \mu\text{g mL}^{-1}$) and relaxation times was measured. Another phantom at the same concentration of unlabeled cells was also used as a control. All the phantoms had a cylindrical shape and were about 1.5 cm long. The total amount of Gd^{3+} ions in each of the phantoms was evaluated by ICP-AES. The average uptake of Gd^{3+} ion by each cell was calculated from the concentration of Gd^{3+} ions and the total number of cells. The analysis was performed in triplicate, and the means and standard deviations of the results were calculated.

Biodistribution studies

To study the biodistribution of GSN and Magnevist® (Bayer HealthCare Pharmaceuticals, Inc, Montville, NJ, USA) in tumor or nontumor tissues, 0.2 mmol kg^{-1} was injected (intravenously) into the mice. After different time intervals (10 minutes and 30 minutes) postinjection, the tumor, kidney, heart, and gastrointestinal tissues of animals were removed and their Gd^{3+} ions content was determined by ICP-AES analysis. Each experiment was carried out at least three times. For the ICP-AES analysis, the animals were sacrificed and the target samples were collected and weighed. By addition of Ultrapure nitric acid (Sigma-Aldrich) (1.00 mL, 70%; EMD Millipore, Billerica, MA, USA) to the samples, as well as centrifugation of the prepared solutions after 2 days, the supernatant was removed and diluted with water and used for the next step of Gd^{3+} determination using ICP-AES (Optima 3100XL; PerkinElmer).²⁰

MR measurement

Relaxation time rates of GSN were measured at different concentrations, using different spin echo and gradient echo protocols in 3T MRI (Siemens AG, Munich, Germany) with a head coil. For T_2 measurements, multiple spin echo protocols were used. In total, 32 echoes with an echo spacing of 2 ms were obtained. The first echo time was 13.2, the repetition time was 3000 ms (matrix = 256×256), and the slice thickness was 1.5 mm and nonaveraged. A FLASH protocol was used to compute T_1 maps. Repetition times were 20 ms, 50 ms, 100 ms, 200 ms, 400 ms, 600 ms, 1000 ms, 2000 ms, and 3000 ms. The first echo time was 12 ms (matrix = 256×256), and the slice thickness was 1.5 mm and nonaveraged.

Cancer cells imaging

For cancer cell imaging, 5×10^3 labeled cells per pellet with a volume of 0.1 mL (subcutaneous) were injected into the

dorsal flank of a male BALB/c mouse. Another equivalent amount of unlabeled cell pellets was also injected into right side as the control. The animal was then immediately transferred to 3 Tesla MRI for imaging.

Statistical analysis

Multigroup comparisons of the means were analyzed by a one-way analysis of variance. Statistical significance for all tests was set at $P < 0.05$. Results were expressed as the mean \pm standard deviation ($n = 3-5$).

Results

Cell toxicity

Figure 1 shows the cell viability using MTT assay on the HT 29 cell line. As shown in Figure 1, GSN-labeled cells had insignificant differences in cell viability at concentrations of $10 \mu\text{g mL}^{-1}$, $30 \mu\text{g mL}^{-1}$, $60 \mu\text{g mL}^{-1}$, and $90 \mu\text{g mL}^{-1}$ for 24 hours ($P < 0.05$).

Inductively coupled plasma results

Inductively coupled plasma results indicated an average cellular uptake of $0.7 \pm 0.09 \text{ pg Gd}^{3+}$ per cell.

Flow cytometry

As shown in Figure 2, more than 70% of the cells were labeled after incubation with GSN-FITC within 2 hours. This indicates that GSN could be readily internalized into

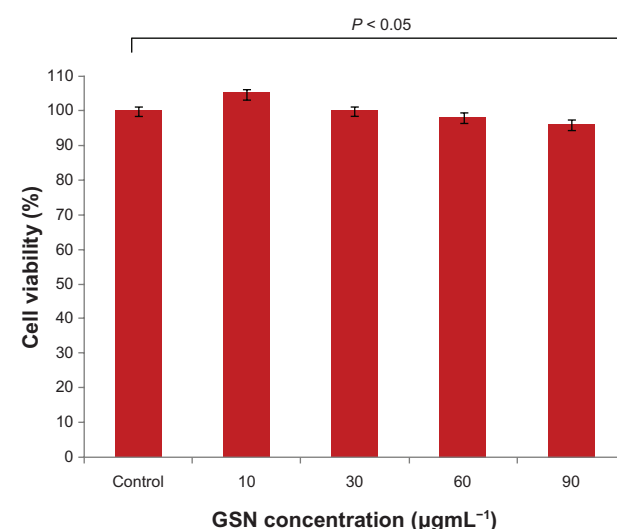


Figure 1 MTT results of 48 hours of GSN exposure to the HT 29 cell line (human colon adenocarcinoma).

Notes: The in vitro cytotoxicity of GNS was examined at four different concentrations. Each concentration was performed in triplicate and the mean \pm standard deviation was shown. GSN-labeled cells had insignificant differences in cell viability at these concentrations ($P < 0.05$).

Abbreviations: GSN, glycosylated silica nanoprobe; MTT, 3-(4,5-Dimethylthiazol-2-yl)-2,5-diphenyltetrazolium bromide.

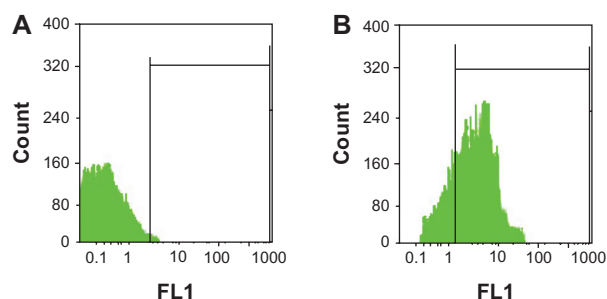


Figure 2 Flow cytometric data on the HT 29 cells.

Notes: The insets show the purity of the cell populations. (A) 1×10^6 HT 29 cells in mL media; (B) 0.6% GSN-labeling cell after 1 hour.

Abbreviations: FL, fluorescent; GSN, glycosylated silica nanoprobe.

the cells within a relatively short incubation time. This high uptake is related to the increased demand for glucose among tumor cells.

Fluorescent microscopic study

The uptake of GSN by the HT 29 cell line was investigated using fluorescence microscopy. The red color of GSN loaded with fluorescent dye (GSNF) could clearly be seen in Figure 3. The result indicates that the nanoparticles were internalized into the cells.

Relaxivity measurement of GSN in the HT 29 cell line

The relaxation of GSN-labeled cells was characterized by 3 Tesla MRI. Figure 4 shows the relaxation rates of GSN-labeled cells. The r_1 relaxivity of GSN-labeled cells was $12.9 \pm 1.6 \text{ mM}^{-1}\text{s}^{-1}$. The fitted curves for the R_1 volume was near 1, indicating that the relaxation rate curve was an excellent fit for the measured data.

In vitro MRI imaging

Figure 5 shows the r_1 and R_2 relaxation rates for an increasing number of labeled cells (1×10^6 , 3×10^6 , 5×10^6 , and 7×10^6 cells). The results showed that $1/T_1$ effects increased linearly with the increasing number of labeled cells. This result was confirmed by the ICP-AES results.

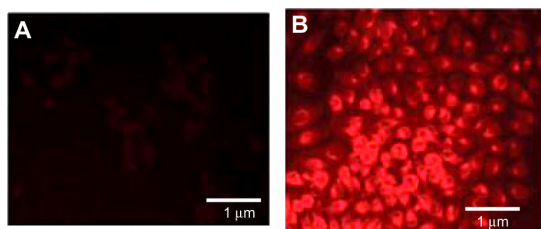


Figure 3 Fluorescent microscopic images.

Notes: (A) Images of unlabeled HT 29 cell lines. (B) Red fluorescence images of the labeled cells.

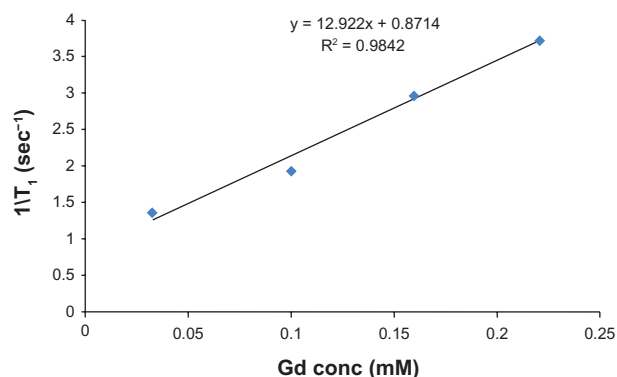


Figure 4 r_1 relaxivity measurement in labeled HT 29 cell lines.

Abbreviations: T_1 , longitudinal relaxation time; Gd conc, gadolinium concentration (mM).

Biodistribution

Figure 6 shows the percentage of Gd^{3+} ions in different tissues, including tumor tissues. The results showed a high GSN accumulation in tumor tissues compared to Magnevist®. The tumor accumulation was time dependent; the accumulation levels of GSN 10 minutes and 30 minutes after injection were 24% and 45%, respectively, which were higher than those of Magnevist® accumulation in tumor tissues (11% [10 minutes] and 5% [30 minutes]). Biodistribution data of the other tissues is illustrated in Figure 6.

Cancer cell imaging

For cell imaging, we injected about 5×10^3 labeled cells and 5×10^3 unlabeled cells in the right and left dorsal flank of mice, respectively. Figure 7 showed that the labeled cells had very good signals after 20 minutes when compared to the unlabeled cells.

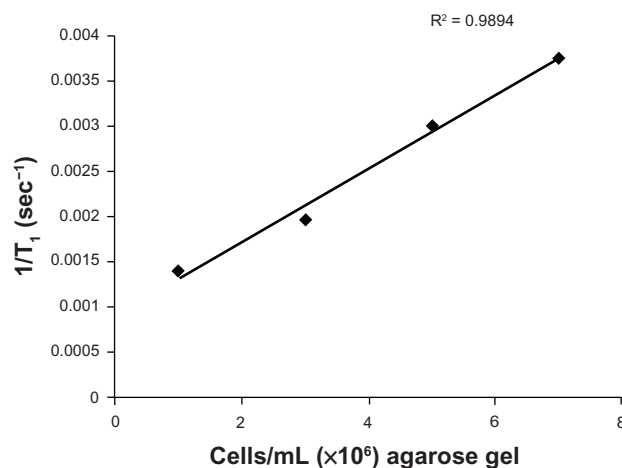


Figure 5 $1/T_1$ relaxation time measurements of GSN-labeled HT 29 cell lines with increasing number of labeled cells in 1.0% agarose gel.

Note: Error bars represent one standard deviation.

Abbreviation: GSN, glycosylated silica nanoprobe.

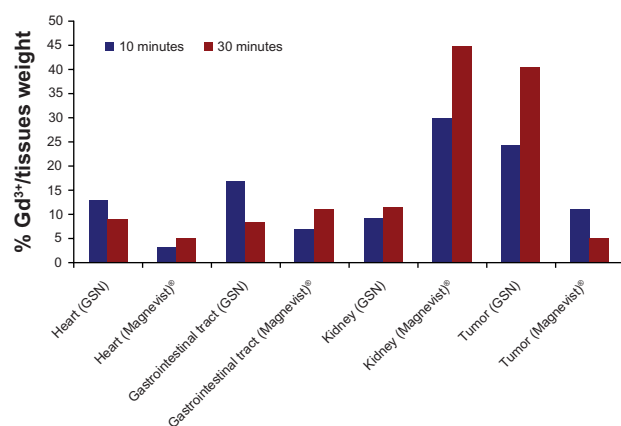


Figure 6 Biodistribution study of GSN and Magnevist® in some critical tissues (heart, gastrointestinal tract, kidney, and tumor) 10 minutes and 30 minutes postinjection.

Abbreviations: Gd³⁺, lanthanide gadolinium; GSN, glycosylated silica nanoprobe.

Discussion

Cancer cells have an increased demand for glucose, which is met by increased availability of glucose through vasculogenesis and through enhanced cellular entry of glucose through the upregulation of specific transporters (GLUT1 and SGLT1).⁸ The rate of glucose entry into cancer cells is at least 20–30-fold higher than in normal cells. This unique

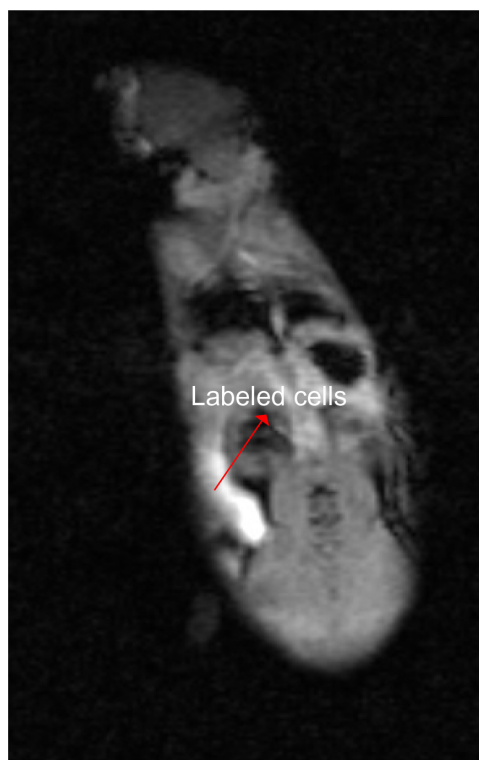


Figure 7 Injection of $\sim 5 \times 10^3$ labeled cells and $\sim 5 \times 10^3$ unlabeled cells in the right and left dorsal flank of mice, respectively.

Note: The labeled cells (arrow) had very good signals after 20 minutes compared to the unlabeled cells.

phenomenon is the basis for the use of glycosylated nanoparticles for cell imaging.⁸ The GSN serves as the MRI probe.

In the present study, intracellular uptake of GSN by ICP-AES was quantified and qualified using flow cytometry and fluorescent microscopy, respectively. The intracellular uptake of GSN was also studied based on transverse relaxations (r_1) in vitro, with increasing concentration of labeled cells dispersed in homogenous phantoms. The in vitro studies on human colon adenocarcinoma (HT 29 cell line) showed that the GSN is taken up by cells two to seven times more efficiently than MSN-Gd³⁺.

The ICP-AES results showed that the intracellular uptake of GSN in cells was on average 0.76 ± 0.09 pg Gd³⁺ per cell, which was consistent with other studies that used the serine-derivatized carbon nanotube to label the MCF-7 human breast cancer cell line and Gd³⁺-based single-wall carbon nanotube in a mouse macrophage cell line.^{17,18}

The results have shown that HT 29 could also be reliably labeled with GSN, without using a transfection agent or without using advanced labeling techniques. This property can be used for intracellular uptake quantifications and cancer cell imaging.

GSNs are a new biocompatible class of MRI contrast agents. The cytotoxicity studies have shown that GSN-labeled cells exhibited 100% viability when compared to unlabeled controls. A further increase in the concentration would lead to a very low decrease in cell viability at $90 \mu\text{g mL}^{-1}$ Gd³⁺ ions. The results suggested that $90 \mu\text{g mL}^{-1}$ of Gd³⁺ is probably the best concentration used for cell labeling.

The quantitative biodistribution results have revealed that the accumulation of GSN in tumor tissues is much higher than for Magnevist® (Figure 6). The GSN accumulation in tumor tissues 10 minutes and 30 minutes postinjection was 24% and 45%, respectively. However, the Magnevist® accumulations were 11% and 5%, respectively. These results were attributed to the higher demand of cancer tissues for glucose, the increased availability of glucose through vasculogenesis, and the overexpression of GLUTs in cancerous cells.⁸

The relaxivity studies have shown that the r_1 values of GSN-labeled cells was $12.9 \pm 1.6 \text{ mM}^{-1}\text{s}^{-1}$ (Figure 4). The enhanced MR relaxivity is attributed to the easy access of cells' water molecules to Gd³⁺ which have been loaded in GSN. A significant positive signal enhancement in the T_1 -weighted image was observed for the labeled cells when compared to the unlabeled cells (Figure 7). The T_1 -weighted image enhancements were related to the reduction of T_1 relaxation times.¹⁶

Another interesting objective was to enhance the sensitivity of this class of glucose transporter-targeting agents, which relies on the observation that the internalization occurs through receptor-mediated endocytosis. It is likely that upon binding of the modified glucose, the transporting protein is unable to proceed with the successive steps that bring glucose into the cytoplasm; thus, it moves to the clathrin-rich region to be entrapped in an endosomal vesicle. However, to carry enough imaging contrast agent to the target site, we used MSN loaded with Gd^{3+} chelates, whose size limited the access only to the glucose transporters on the endothelial walls of the tumor tissue.

In summary, GSN displays several positive features; its small size allows for its easy diffusion into the tissue to reach the surface of the tumor cells. It is internalized by receptor-mediated endocytosis, thus avoiding undesirable interactions with the molecules of the cytoplasm. Clearly, targeting glucose transporters with small, stable GSN appears to be a more efficient route for an improved delineation of the pathological tissue.

Conclusion

The large and linear transverse relaxation of GSN provides these contrast agents with good sensitivity for cellular imaging in 3 Tesla MRI. Future research may be needed to study the cellular uptake and distribution mechanisms of GSN and its subcellular localization.

Acknowledgments

This paper is a major part of a PhD thesis in nanomedicine by Bita Mehravi. Financial support was provided by Shahid Beheshti University of Medical Sciences and the Tehran University of Medical Sciences.

Disclosure

The authors report no conflicts of interest in this work. The authors declare no competing financial interest.

References

1. National Cancer Institute. International cancer screening network [webpage on the Internet]. Bethesda, MD: National Cancer Institute; 2008 [updated December 11, 2012]. Available from: <http://appliedresearch.cancer.gov/icsn/colorectal/mortality.html>. Accessed.
2. Raymond KN, Pierre VC. Next generation, high relaxivity gadolinium MRI agents. *Bioconjug Chem*. 2005;16(1):3–8.
3. Ananta JS, Godin B, Sethi R, et al. Geometrical confinement of gadolinium-based contrast agents in nanoporous particles enhances T1 contrast. *Nat Nanotechnol*. 2010;5(11):815–821.
4. Slowing II, Vivero-Escoto JL, Wu CW, Lin VS. Mesoporous silica nanoparticles as controlled release drug delivery and gene transfection carriers. *Adv Drug Deliv Rev*. 2008;60(11):1278–1288.
5. Shen Z, Li Y, Kohama K, O'Neill B, Bi J. Improved drug targeting of cancer cells by utilizing actively targetable folic acid-conjugated albumin nanospheres. *Pharmacol Res*. 2011;63(1):51–58.
6. del Amo EM, Urtti A, Yliperttula M. Pharmacokinetic role of L-type amino acid transporters LAT1 and LAT2. *Eur J Pharm Sci*. 2008;35(3):161–174.
7. Sun C, Lee JS, Zhang M. Magnetic nanoparticles in MR imaging and drug delivery. *Adv Drug Deliv Rev*. 2008;60(11):1252–1265.
8. Ganapathy V, Thangaraju M, Prasad PD. Nutrient transporters in cancer: relevance to Warburg hypothesis and beyond. *Pharmacol Ther*. 2009;121(1):29–40.
9. De la Fuente JM, Penadés S. Glyconanoparticles: types, synthesis and applications in glycoscience, biomedicine and material science. *Biochim Biophys Acta*. 2006;1760(4):636–651.
10. Amanlou M, Siadat SD, Ebrahimi SE, et al. $Gd(3+)$ -DTPA-DG: novel nanosized dual anticancer and molecular imaging agent. *Int J Nanomedicine*. 2011;6:747–763.
11. Veerapandian M, Yun K. Synthesis of silver nanoclusters and functionalization with glucosamine for glyconanoparticles. *Synthesis and Reactivity in Inorganic, Metal-Organic, and Nano-Metal Chemistry*. 2010;40(1):56–64.
12. Rojo J, Diaz V, de la Fuente JM, et al. Gold glyconanoparticles as new tools in antiadhesive therapy. *Chembiochem*. 2004;5(3):291–297.
13. Burtea C, Laurent S, Colet JM, Vander Elst L, Muller RN. Development of new glycosylated derivatives of gadolinium diethylenetriaminepentaacetic for magnetic resonance angiography. *Invest Radiol*. 2003;38(6):320–333.
14. Bayly SR, Fisher CL, Storr T, Adam MJ, Orvig C. Carbohydrate conjugates for molecular imaging and radiotherapy: 99m Tc(I) and 186Re(I) tricarbonyl complexes of N-(2'-Hydroxybenzyl)-2-amino-2-deoxy-D-glucose. *Bioconjug Chem*. 2004;15(4):923–926.
15. Mehravi B, Ahmadi M, Amanlou M, et al. Facile conjugation of glucosamine on Gd^{3+} based nanoporous silica using heterobifunctional crosslinker (ANB-NOS) for cancer cell imaging. *Int J Nanomedicine*. 2013;8:1–12.
16. Taylor KM, Kim JS, Rieter WJ, An H, Lin W, Lin W. Mesoporous silica nanospheres as highly efficient MRI contrast agents. *J Am Chem Soc*. 2008;130(7):2154–2155.
17. Hassaan AA, Chan BT, Tran LA, et al. Serine-derivatized gadonanotubes as magnetic nanoprobe for intracellular labeling. *Contrast Media Mol Imaging*. 2010;5(1):34–38.
18. Tang AM, Ananta JS, Zhao H, et al. Cellular uptake and imaging studies of gadolinium-loaded single-walled carbon nanotubes as MRI contrast agents. *Contrast Media Mol Imaging*. 2011;6(2):93–99.
19. Estévez MC, O'Donoghue MB, Chen X, Tan W. Highly fluorescent dye-doped silica nanoparticles increase flow cytometry sensitivity for cancer cell monitoring. *Nano Res*. 2009;2:448–461.
20. Shen Y, Shao Y, He H, et al. Gadolinium(3+)-doped mesoporous silica nanoparticles as a potential magnetic resonance tracer for monitoring the migration of stem cells in vivo. *Int J Nanomedicine*. 2013;8:119–127.

International Journal of Nanomedicine**Dovepress****Publish your work in this journal**

The International Journal of Nanomedicine is an international, peer-reviewed journal focusing on the application of nanotechnology in diagnostics, therapeutics, and drug delivery systems throughout the biomedical field. This journal is indexed on PubMed Central, MedLine, CAS, SciSearch®, Current Contents®/Clinical Medicine,

Journal Citation Reports/Science Edition, EMBase, Scopus and the Elsevier Bibliographic databases. The manuscript management system is completely online and includes a very quick and fair peer-review system, which is all easy to use. Visit <http://www.dovepress.com/testimonials.php> to read real quotes from published authors.

Submit your manuscript here: <http://www.dovepress.com/international-journal-of-nanomedicine-journal>